AUTOIGNITION OF JET PROPULSION FUEL AND ITS SURROGATE: EXPERIMENTS AND MODELING

V. Ya. Basevich, A. A. Borisov, S. M. Frolov, G. I. Skachkov, and K. Ya. Troshin

N. N. Semenov Institute of Chemical Physics
Russian Academy of Sciences
Moscow 119991, Russia

1 Introduction

Jet propulsion fuels like Jet-A, JP-10, TS-1, etc. are considered as candidate fuels for advanced propulsion systems including pulse detonation engines (PDE). For PDE applications, there is a need in experimental data on spontaneous ignition of the fuels in the whole range of operating conditions. For simulation purposes, jet propulsion fuels are usually represented by multicomponent blends of primary hydrocarbons. For example, Jet-A and its Russian analog TS-1 are modeled by blends containing *n*-decane (73%), *n*-hexane (9.1%), and benzene (18.2%) [1]. Reliable data on high-temperature ignition delays of jet propulsion fuels and the components of the corresponding surrogate fuels in air are available, which is not the case with the low-temperature data. However, verification of kinetic mechanisms to be used in simulating dynamics of deflagration-to-detonation transition (DDT) or shock-to-detonation transition (SDT) processes in fuel–air mixtures requires information about representative reaction times in the whole range from few microseconds to seconds. Plotting of the measured ignition delays within as wide as possible range would allow one to avoid far extrapolation of the data and significant mistakes associated with such extrapolation. This is of particular importance because data reported by various authors cover narrow temperature ranges and the slopes of the Arrhenius plots are assessed with significant mistakes. Therefore, one of the goals

of this study is to supplement with low-temperature data the high-temperature data provided by shock-tube measurements. The other goal is to develop compact reaction mechanisms describing the ignition kinetics of multicomponent surrogates of the jet propulsion fuels.

2 Experiments

2.1 Static apparatus

Low-temperature data were obtained in a static apparatus designed and manufactured for these measurements. Ignition delays measured in the apparatus covered the range 0.2–10 s, which corresponded to temperatures below 1000 K for majority of hydrocarbons. The gas mixture studied was rapidly admitted through an electromagnetically driven valve into the reactor evacuated and preheated to a preset temperature. The lower value of ignition delays measured by this technique was limited by the mixture preheat time. Measurements with thermocouples of the temperature distribution in the reactor showed that preheating of the major gas portion in the reactor to the temperature of its walls was completed within 0.1–0.2 s, which was slightly longer than the valve opening time. Ignition delay was measured as a time elapsed after the instant of mixture preheating to the temperature of reactor walls to an abrupt rise of pressure recorded with a pressure gauge.

The schematic of the apparatus is shown in Fig. 1. The reactor was a stainless steel cylinder 10 cm i.d. and 10 cm in height. The temperature of its walls was controlled with a thermocouple inserted in a channel drilled in the wall. Gaseous mixtures were admitted from storage vessel (*9*) 2 l in volume which was also equipped with an electric heater. Pressure gauge *6* monitored both filling the reactor with gas and self-ignition process.

Studies of ignition of liquid fuels required modification of both the apparatus and the procedure of performing tests. Premixing of the mixture components in this case necessitated preheating of the storage vessel; however, the tube connecting this vessel and reactor and the valve and its nest were not preheated; therefore, liquid fuel would condense on the cold metal surfaces. In the first version of experiment implementation, a desired amount of liquid fuel was injected with a hypodermic syringe underneath the valve plunger. Air in the storage

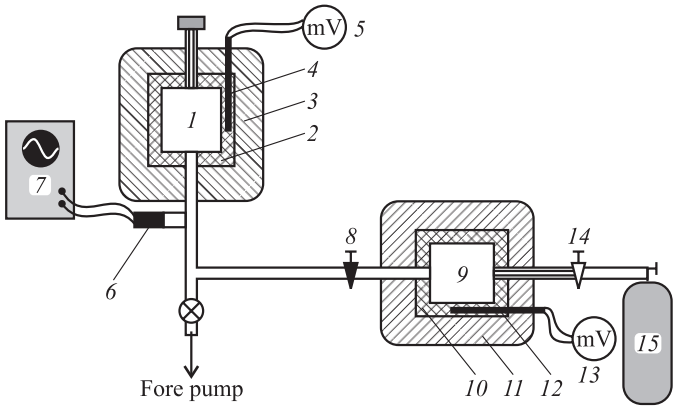

Figure 1 Schematic of the static apparatus: *1* — reactor, *2* — electrical furnace, *3* — thermal insulation, *4* — thermocouple, *5* — millivoltmeter, *6* — pressure gauge, *7* — recording system including analog-to-digital converter and PC, *8* — fast operating electromagnetic valve, *9* — vessel with mixture, *10* — electrical heater, *11* — thermal insulation, *12* — thermocouple, *13* — millivoltmeter, *14* — valve, and *15* — mixer

vessel was preheated to 150 or 200 °C and pressurized to the amount needed to fill the reactor to a desired pressure level after opening the valve. Air flow entrained the fuel and delivered it to the reactor in the form of a homogeneous mixture.

This experimental procedure was used to measure ignition delays of stoichiometric kerosene TS-1 – air mixtures at different pressures. Pressure records exhibited a two-stage behavior: after the pressure rise in the course of mixture admittance, the signal leveled off and then exhibited a step-wise rise which was followed by a peak indicating main explosion.

Further studies have suggested that most likely the observed pressure signal resulted from peculiarities of fuel distribution in the reactor (which was not necessarily homogeneous with such an imperfect mixture preparation procedure) rather than from cool-flame premature ignition. Therefore, the experimental procedure was changed. First, a measured fuel portion was introduced with a hypodermic syringe in the evacuated reactor and then, within no more than a second, preheated

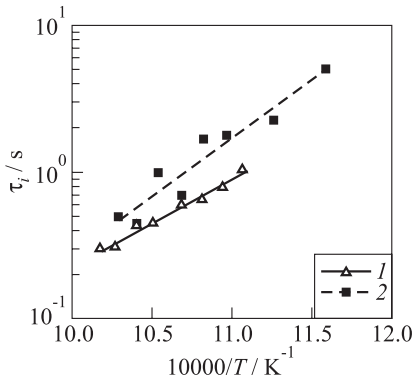

Figure 2 Comparison of ignition delays of propane–air mixtures measured in the reactor with two different techniques of fuel and air injection: triangles (*1*) pertain to tests with injection of premixed components, squares (*2*) are ignition delays measured in tests with separate injection of the fuel and air

air was admitted in it to the preset pressure. The amount of fuel injected was additionally checked by the pressure record which showed a small step-wise pressure rise before the major one due to air injection. The ratio between the first and second pressure rise amplitudes always corresponded to the preset fuel–air ratio. Remarkably, the two-stage pressure signal was completely eliminated by the new procedure of injection of the mixture components.

Thus, based on the physical reasoning and obtained results, it is believed that separate injection of the mixture components in the reactor was the most suitable procedure providing adequate data on ignition delays of liquid fuels, because it precluded fuel losses due to sticking to the walls, imperfect mixing of the components and faster and more homogeneous preheating of the mixture. The data corresponded to homogeneous vapor–air mixtures and could be used in kinetic analyses.

To make it sure that mixing of the separately injected components did not introduce significant changes in the measured ignition delays (e.g., because of partial pyrolysis of the fuel or not enough rapid mixing in the reactor), the results of measurements performed by two techniques for ignition of purely gaseous propane–air mixture were com-

pared. Experiments in which either premixed propane–air mixture was injected in the reactor or propane and air were injected one after the other were performed in the same reactor under the identical conditions. The results are compared in Fig. 2. As seen, although the separate injection of components yields slightly greater ignition delays (presumably because the fuel–air mixing time was longer than the time needed to ignite premixed gases entering the reactor near its walls), the discrepancy between the data obtained by different techniques is comparable with the scatter of individual sets of data.

The focus of this study is the low-temperature ignition performance of TS-1 and its surrogate containing *n*-decane (73%), *n*-hexane (9.1%), and benzene (18.2%) [1]. Therefore, the liquid fuels tested with the use of separate injection of the fuel and air were: *n*-decane, *n*-hexane, benzene, and TS-1. Initial pressures varied from 1 to 8 atm.

2.2 *n*-Decane

Stoichiometric *n*-decane–air mixtures were ignited in the static apparatus at initial pressures from 1 to 8 atm and initial temperatures from 550 to 630 K. Experiments revealed that the ignition delays in these temperature and pressure ranges were pressure independent and fitted quite well to a linear Arrhenius dependence. Figure 3 compares the present experimental data with those available in the literature. Curves in Fig. 3 correspond to the overall reaction mechanism of *n*-decane oxidation discussed below in Section 3. As seen from Fig. 3, there are three domains in the $\log(\tau)$ vs. $1/T$ plot. The effective activation energy in the low- and high-temperature domains are quite close to each other. The domain of the Negative Temperature Coefficient (NTC) is observed at ignition delays between 10^{-3} and 10^{-2} s and covers quite a wide temperature range. The trend seen in Fig. 3 suggests that the NTC temperature interval narrows as the pressure decreases.

2.3 *n*-Hexane

The results of measurements of ignition delays of stoichiometric *n*-hexane–air mixtures at temperatures 550–663 K and pressures 1 and 2.5 atm are shown in Fig. 4 by closed triangles. Again, the ignition delays exhibit a weak pressure dependence within the interval tested.

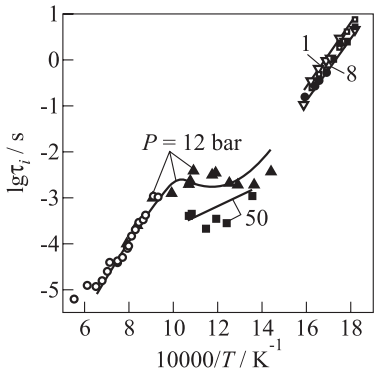

Figure 3 Ignition delays of the stoichiometric n-decane–air mixture within experimental ranges of pressure and temperature tested in available literature. Experimental data at pressures from 1 to 8 bar correspond to present experiments, the data at 12 and 50 bar correspond to [2]; circles correspond to [1]. Solid curves correspond to the predictions by the overall mechanism

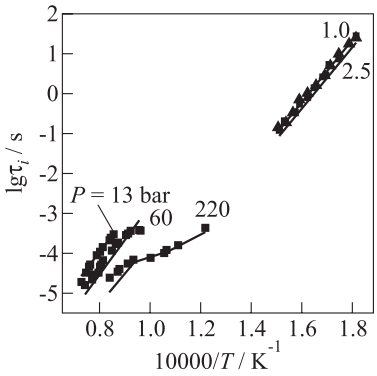

Figure 4 Ignition delays of n-hexane–air mixture within experimental ranges of pressure and temperature tested in available literature. Experiments at 1 and 2.5 bar correspond to present data for the stoichiometric mixture; experiments at 13, 60, and 220 bar correspond to fuel-lean mixture with a fuel–air ratio $\Phi = 0.5$ reported in [3]. Solid curves correspond to the predictions by the overall mechanism

Figure 4 also compares the results of present measurements with the literature data. The gap between the low- and high-temperature data suggests that it is in this very temperature range where one could expect NTC. Curves in Fig. 4 correspond to the overall reaction mechanism of n-hexane oxidation discussed below in Section 3.

2.4 Benzene

The results of measurements of ignition delays of stoichiometric benzene–air mixtures at temperatures 936–1013 K and pressure 3 atm are shown in Fig. 5 by squares. Figure 5 also compares the results of present measurements with the literature data [4]. Curves in Fig. 5 correspond to the overall reaction mechanism of benzene oxidation discussed below in Section 3.

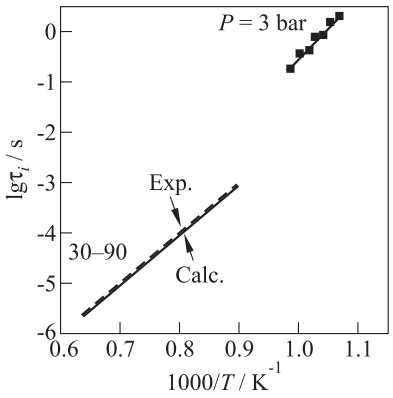

Figure 5 Ignition delays of the stoichiometric benzene–air mixture. Experiments at 3 bar (squares) correspond to present data; experimental data at 30 to 90 bar (dashed line) are taken from [4]. Solid curves correspond to the predictions by the overall mechanism

2.5 Kerosene TS-1

Ignition delays of stoichiometric kerosene TS-1 – air mixtures measured at temperatures 850–950 K and pressure of 1 atm are shown in Fig. 6.

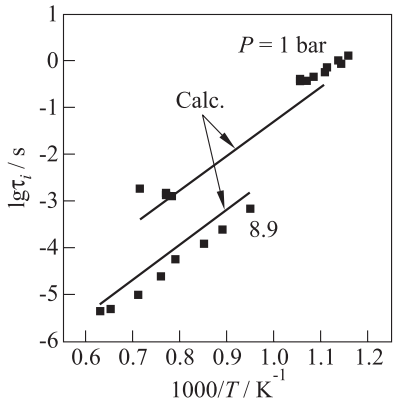

Figure 6 Ignition delays of the stoichiometric kerosene TS-1 – air mixture. Experimental points at 1 bar correspond to present data; points at 8.9 bar correspond to experiments [1] for Jet-A. Solid lines correspond to the predictions by the overall mechanism for the surrogate fuel containing 73% *n*-decane, 9% *n*-hexane, and 18% benzene

Also shown in Fig. 6 is the comparison with the available literature data. The effective activation energies of the Arrhenius plots of low- and high-temperature ignition delays are close to each other. Curves in Fig. 6 correspond to the overall reaction mechanism of kerosene oxidation discussed below in Section 3. Kerosene TS-1 was represented as a surrogate fuel containing 73% *n*-decane, 9% *n*-hexane, and 18% benzene [1].

3 Overall Reaction Mechanism

The following overall mechanism of fuel oxidation containing 5 reactions and 6 species was used to approximate the experimental data of Figs. 3 to 6 [5, 6]:

$$C_nH_m + (0.5n + 0.25m)O_2 \rightarrow nCO + 0.5mH_2O \quad (1)$$

$$H_2 + H_2 + O_2 \rightarrow 2H_2O \quad (2)$$

$$CO + CO + O_2 \rightarrow CO_2 + CO_2 \quad (3)$$

$$CO + H_2O \rightarrow CO_2 + H_2 \qquad (4)$$

$$CO_2 + H_2 \rightarrow CO + H_2O \qquad (-4)$$

The rates of reactions (1)–(4,-4) were determined by the relationship

$$w_i = A_i \exp\left(-\frac{E_i}{RT}\right) \prod_j n_{ij}$$

written in terms of standard notations. The rate of reaction (1) was found from the relationship for the bimolecular reaction:

$$w_1 = A_1[C_nH_m][O_2] \exp\left(-\frac{E_1}{RT}\right), \quad A_1 = A_{01}P^{n_1}$$

where $[C_nH_m]$ and $[O_2]$ are the molar concentrations of fuel and oxygen.

To model multistage autoignition, the approach similar to [7] was used. The preexponential factor A_1 and activation energy E_1 of reaction (1) at low and high temperatures were determined independently of each other by fitting the predicted and measured ignition delay dependencies on temperature. To separate the "low-temperature" branch of the ignition delay curve from the "high-temperature" branch, the concept of transition temperature T_* was introduced. It was assumed that at $T < T_*$, parameters A_1 and E_1 were equal to their low-temperature values A_{1u}, n_{1u}, and E_{1u}, whereas at $T \geq T_*$, they were equal to their high-temperature values A_{1h}, n_{1h}, and E_{1h}. Preexponential factors A_{1u} and A_{1h} were assumed to depend on pressure P as

$$A_{1u} = A_{01u}P^{n_{1u}}; \quad A_{1h} = A_{01h}P^{n_{1h}}$$

where A_{01u}, A_{01h}, n_{1u}, and n_{1h} are the constants.

For reactions (2) to (4,-4), the preexponential factors and activation energies were not changed during transition through T_* and were taken the same as in [5, 6]. Thus, during transition through T_*, only parameters A_1 and E_1 were changed. The kinetic parameters of reaction (1) and the recommended values of the transition temperature T_* for n-decane, n-hexane, and benzene are presented in Table 1. Table 2 shows the kinetic parameters of reactions (2) to (4,-4).

Note that at high initial temperatures, the overall reaction mechanism (1) to (4,-4) has to be supplemented by additional two dissociation-like reactions and one species (see [6]). To model self-ignition of kerosene

Table 1 Recommended values of kinetic parameters of reaction (1) for n-decane, n-hexane, and benzene

Fuel	A_{01u}, 1/(mole·s)	n_{1u}	E_{1u}, kcal/mole	T_*, K	A_{01h}, 1/(mole·s)	n_{1h}	E_{1h}, kcal/mole
n-$C_{10}H_{22}$	$1.1 \cdot 10^{14}$	−0.743	36.7	1000	$5.16 \cdot 10^{11}$	0.383	45
n-C_6H_{14}	$1.167 \cdot 10^{15}$	−0.743	40.8	1074	$3.81 \cdot 10^{12}$	−0.0804	45
C_6H_6	$3.03 \cdot 10^{15}$	0	66	1069	$9.22 \cdot 10^{13}$	−0.14	57.8

Table 2 Kinetic parameters of reactions (2) to (4,-4) [5, 6]

No.	Reaction	A, l, mole, s	E, kcal/mole
2	$H_2 + H_2 + O_2 = H_2O + H_2O$	$7.0 \cdot 10^{13} P^{-0.5}$	21.0
3	$CO + CO + O_2 = CO_2 + CO_2$	$8.5 \cdot 10^{12} P^{-1.5}$	21.0
4	$CO + H_2O = CO_2 + H_2$	$1.0 \cdot 10^{12} P^{-1}$	41.5
−4	$CO_2 + H_2 = CO + H_2O$	$3.1 \cdot 10^{13} P^{-1}$	49.1

surrogate of Section 2.5, the overall mechanism was composed of three reactions (1) for n-decane, n-hexane, and benzene, and a single set of reactions (2) to (4,-4). The initial concentrations of the surrogate components were taken according to the recommended composition: 73% n-decane + 9% n-hexane + 18% benzene.

The comparison of predicted and measured results for jet propulsion kerosene presented in Fig. 6 indicates that the agreement between predictions and measurements is satisfactory.

Concluding Remarks

Simulation of DDT or SDT processes in fuel–air mixtures requires information about representative reaction times in the range from few microseconds to seconds. The experimental studies reported in this paper provide missing low-temperature ignition delays for n-decane, n-hexane, benzene, and kerosene TS-1. In addition, the paper provides a compact overall oxidation mechanism for the listed hydrocarbons valid for both

low- and high-temperature conditions. The mechanism was proved to be readily applicable for modeling self-ignition of fuel blends, in particular, those representing a jet propulsion kerosene. Further studies are worth to be focused on ignition of the listed fuels in the temperature range corresponding to NTC. Also, pressure and concentration dependences of the ignition delays in the entire temperature range have to be ascertained.

Acknowledgments

This work was performed under partial financial support of the IPP Project ANL-T2-220-RU, sponsored by the U.S. Department of Energy IPP Program, and Russian Foundation for Basic Research grants 05-08-18200a, 05-0850115a, and 05-08-33411a.

References

1. Dean, A. J., O. G. Penyazkov, K. L. Sevruk, and B. Varatharajan. 2005. Ignition of aviation kerosene at high temperatures. *20th Colloquium (International) on the Dynamics of Explosions and Reactive Systems*. Montreal, Canada. CD.
2. Toland, A., and J. M. Simmie. 2003. Ignition of alkyl nitrate/oxygen/argon mixtures in shock waves and comparisons with alkanes and amines. *Combustion Flame* 132:556–64.
3. Zhukov, V. P., V. A. Sechenov, and A. Yu. Starikovskii. 2004. Ignition delay times in lean n-hexane–air mixture at high pressures. *Combustion Flame* 136:257–59.
4. Kogarko, S. M., and A. A. Borisov. 1960. *Izv. Akad. Nauk SSSR, OkhN* 8:134.
5. Frolov, S. M., V. Ya. Basevich, M. G. Neuhaus, and R. Tatschl. 1997. A joint velocity–scalar PDF method for modeling premixed and nonpremixed combustion. In: *Advanced computation and analysis of combustion*. Eds. G. Roy, S. Frolov, and P. Givi. Moscow: ENAS Publ. 537–61.
6. Basevich, V. Ya., A. A. Belyaev, and S. M. Frolov. 1998. *Rus. J. Chemical Physics* 17(9):112.
7. Basevich, V. Ya., S. M. Frolov, and H. J. Pasman. 2005. Overall reaction mechanism of two-stage n-butane oxidation. In: *Nonequilibrium processes. Volume 1: Combustion and detonation*. Eds. G. Roy, S. Frolov, and A. Starik. Moscow: TORUS PRESS. 25–29.